Jurnal Riset Kimia

ISSN (print) : 1978-628X
ISSN (online) : 2476-8960

Synthesis of Mg-doped TiO_2 using A Hydrothermal Method as Photoanode on Bixin-Sensitized Solar Cell

Winda Rahmalia[1*], Intan Syahbanu[1], Nurlina[1], Ayu Widya Sari[1], Septiani[1]
[1]Department of Chemistry, Faculty of Mathematics and Natural Science, Tanjungpura University, Pontianak, West Kalimantan, Indonesia

Corresponding Author:
Winda Rahmalia
winda.rahmalia@chemistry.untan.ac.id

Received: July 2023
Accepted: September 2023
Published: September 2023

Abstract

Titanium dioxide (TiO_2) with magnesium (Mg) doping for dye-sensitized solar cell (DSSC) photoanode application has been synthesized. DSSC components used in this study were photosensitizer (bixin), electrolyte (I^-/I_3^-), cathode (platinum), and photoanode (Mg-TiO_2). This research aims to determine the characteristics of Mg-doped TiO_2 photoanode with variations in dopant concentration based on the results of XRD and DR/UV-Vis analysis, as well as to determine the maximum efficiency conversion energy of DSSC using Mg-doped TiO_2 and undoped TiO_2 as photoanodes. The synthesis of TiO_2 and Mg-TiO_2 was carried out using the hydrothermal method with variations in the concentration of Mg dopant of 0, 0.5, 1, and 2% based on the molar ratio. The presenceof 2% of Mg in anatase TiO_2 paste decreased the TiO_2 band gap from 3.15 to 2.60 eV. Analysis results show that adding Mg dopant decreased the crystal size. Mg dopants on TiO_2 could also form new energy levels, which reduced the band gap energy of TiO_2. In addition, the increased concentration of Mg dopants also shifted the absorption capacity of TiO_2 from the ultra-violet (UV) wavelengths region to the visible light area. The maximum energy conversion efficiency of the DSSCs with Mg-doped TiO_2 photoanode of 0.5, 1, and 2% are 0.045; 0.070, and 0.172%, respectively, where these three efficiency values are higher than undoped TiO_2 (0.017%). The results proved that the presence of Mg dopants on the TiO_2 photoanode can increase the efficiency of DSSC.

Keywords: b*ixin; DSSC; Mg doping; photoanode; band gap energy.*

Introduction

Dye-sensitized solar cells (DSSCs) are third-generation photovoltaic cells that convert visible light into electrical energy. The essential components of DSSC consist of conductive transparent glass, a counter electrode, a semiconductor photoanode, an electrolyte, and a dye[1]–[3]. Titanium dioxide (TiO_2) is a photoanode widely used in DSSC. It has a good chemical stability under irradiation[4]. However, this material can only absorb solar ultraviolet light because it has a wide band gap energy (ranging from 3.0 to 3.2 eV). It has a low absorption efficiency because only about 5% of sunlight is emitted in the area. The wide band gap energy also affects the excitation process of electrons from the valence band to the conduction band[5]. The high recombination rate inhibits the performance of TiO_2 as a photoanode material[6]. The electron transport process that takes place randomly in the pores of the TiO_2 nanoparticles causes a charge recombination process (electron-hole) which causes the performance of the DSSC to decrease. In this case, photoanode engineering with the aim of making efficient charge

DOI: https://doi.org/10.25077/jrk.v14i2.622

transport is essential to improve the performance of DSSC.

Several efforts have been made to increase electron transport and prevent charge recombination by modifying the TiO_2 surface, one of them by doping other materials to the TiO_2 surface[7]. Some materials that have been used as dopants include ammonia-activated metakaolinite[8], chitosan[9], rare earth[10],[11], transition[12], and alkaline earth[13],[14] metals. Magnesium is one of the metals currently being used as a dopant for TiO_2. Magnesium (Mg) is a low-cost and easy availability metal dopant that can be used to improve photoanode performance. Mg is an alkali metal that can increase light absorption activity in materials and reduce electron recombination. Mg is also the best material that can replace Ti in large quantities and improve injection and electron transport in the material[15],[16]. Therefore, we used Mg as a dopant for TiO_2 in this study.

Several studies state that Mg metal was chosen as a doping material because it has several advantages compared to other types of metal in the same group. Mg has a ion radius value of (0.57 Å) which is smaller and close to the radius of Ti^{4+} (0.68 Å), so that Mg is able to replace some Ti^{4+} cations in the TiO_2 lattice structure [17]. Metal ion Be^{2+} tends to enter interstitial sites because its radius is much smaller, Ca^{2+} is more difficult to substitute for $Ti^{4+,}$ and is able to cause lattice deformation. Other large ions such as Ba^{2+} and Sr^{2+} cannot enter the crystal lattice and only stay on the surface because their cation radius is very large[18]. In addition, Mg which can replace Ti in large quantities can increase electron injection and transport in the material[16].

The method chosen in this study is hydrothermal because it can control nucleation better, the dispersion rate is higher, it is easy to maintain the shape, and the high reaction rate[10],[19]. In addition, the choice of TiO_2 precursor can affect the size and structure of the formed crystals. Karkare[20], reported that the samples prepared using titanium isopropoxide showed film-like structures, whereas those prepared using titanium butoxide showed spherical granules. A red shift of 0.13 eV was observed in the band gap in the case of non-spherical particles compared to spherical ones. Hence, in this work, we used titanium isopropoxide as a precursor.

Khan et al.[6], reported that using Mg-TiO_2 photoanode in DSSC with ruthenium solution (N719) as a dye resulted in an efficiency of 1.68%. DSSC with ruthenium (N_3) dye using TiO_2 doped with Mg was also investigated by Liu[21], resulting in an efficiency of 7.12%, with a current increase of 26.7% compared to undoped TiO_2. These previous studies used synthetic ruthenium dyes, which are toxic, environmentally unfriendly, and expensive. Therefore, the best alternative is to use natural dyes that can be extracted from biological sources, availability, are cost-efficient, non-toxicity, biodegradable, and environmentally friendly.

In this research, we used bixin (methyl hydrogen 9′-cis-6,6′-diapocarotene-6,6′-dioate) as a natural sensitizer. Bixin is a color pigment found in the seeds of the annatto plant (*Bixa orellana* L.)[22]. Bixin is reddish-orange and can absorb light in the visible light region in the wavelength range of 400-500 nm[23],[24]. Among the many types of carotenoids, bixin has a unique structure with a carboxylate group at one end of its conjugation chain. Therefore, bixin can interact chemically with TiO_2 via monodentate ester-type, bidentate chelating, bidentate bridging, H-bonded, or double H-bonded. Rahmalia et al.[8] reported that DSSC with bixin sensitizer had a maximum energy conversion efficiency of 0.08%.

Throughout the literature search that has been carried out, no research has been found that utilizes Mg- TiO_2 as a photoanode of bixin dye-sensitized solar cells. Therefore, this study investigated the effectiveness of Mg-doped TiO_2 based-photoanode for bixin-sensitized solar cells. TiO_2 was doped with Mg in the 0.5, 1, and 2 mol% range. The variation used adopted the research of Liu [21], aimed to determine the effect and variation of the best

dopants concentration on the characteristics of the TiO_2 with different precursor and to increase DSSC performance using natural dye.

Experimental

Materials

Annatto (*Bixa Orellana* L.) seeds obtained from West Kalimantan, Indonesia. Acetonitrile (C_2H_3N, ≥ 99.8%), ethanol (C_2H_5OH), ethyl acetate ($C_4H_8O_2$, ≥99.9%), glacial acetic acid (CH_3COOH), methanol (CH_3OH), n-hexane, potassium iodide (KI), sodium hydroxide (NaOH), TLC F_{254} and triton-x were supplied by Merck. Standard bixin (6-methyl hydrogen (9Z)-6,6'-diapocarotene-6,6'-dioate, >90%), magnesium nitrate hexahydrate ($Mg(NO_3)_2.6H_2O$, ≥99%), 1-methyl-3-propilimidazolium iodide ($C_8H_{13}IN_2$) and titanium(IV)isopropoxide ($Ti[OCH(CH_3)_2]_4$) were supplied by Sigma Aldrich. The other materials like acetone (CH_3COCH_3, ≥99.9%, Mallinckrodt Chemicals), plastisol (Solaronix), transparent conductive oxide (TCO) glass with fluorine-doped tin oxide (FTO) type coated TEC-7 conductive glass (SOLEM) were also used.

Instruments

Spectrophotometer UV-Vis SHIMADZU, FTIR SHIMADZU.

Methods

Preparation of bixin

Bixin extraction from annatto seeds in this study adopted the method of Gómez-Ortíz et al.[24] and Rahmalia et al.[26], which has been modified. Annatto seeds (107 g) were immersed in 200 mL of ethyl acetate in an Erlenmeyer flask, stirred for 1 hour, and filtered. This process was repeated until all the colors were extracted. The extracted filtrate was evaporated at 40°C to minimize solvent. Furthermore, the crude extract was partitioned using n-hexane and methanol. The fraction that was not soluble in n-hexane or methanol was then dried using N_2 gas to remove the solvent so that a dry extract was obtained. The dried extract was analyzed by thin-layer chromatography (TLC) and UV-Vis spectrophotometer.

Synthesis of TiO_2 and Mg-TiO_2

Photoanode was prepared by modifying the method of Ünlü and Mahmut[12]. The procedure begins by mixing 60 mL of deionized water and 5 mL of 1 M NaOH solution, then adding titanium isopropoxide (TTIP) to the mixed solution. After stirring for 30 minutes, the mixture was transferred into a Teflon vessel and placed in a hydrothermal autoclave for hydrothermal reaction at 210°C for 6 hours. The mixture was then cooled until room temperature, then centrifuged at 2000 rpm for 15 minutes. The white TiO_2 precipitate obtained was washed with deionized water and ethanol three times and dried overnight at 80°C. The TiO_2 anatase was obtained by calcining the dried sample at 450°C for 3 hours. The synthesis of Mg-TiO_2 was carried out using a similar procedure by adding 0.5; 1.0; and 2.0% molarity of $Mg(NO_3)_2.6H_2O$ with the composition was 0.04; 0.08; and 0.16 g, respectively, to the mixture before adding TTIP.

Fabrication of dye-sensitized solar cells (DSSCs)

Preparation of transparent conductive oxide (TCO)

TCO glasses measuring 2.5 x 2.0 cm^2 were immersed in 70% ethanol using a bath sonicator for 30 minutes, then dried at 100°C for 1 hour. The conductive side of the glasses was determined using a multimeter [25].

Preparation of photoanode, cathode and electrolyte

Photoanodes and cathodes were prepared by the doctor-blading method. The TiO_2 and Mg-TiO_2 pastes (separately) were deposited on TCO glass with an active side of 1 cm^2 to form photoanodes. The Pt paste was deposited on the others TCO glass to form cathodes. The photoanodes were heated in a furnace at 450°C for 5 minutes. The electrolyte used in this study was a redox pair (I^-/I_3^-). The 1.66 g KI and 0.127 g I_2 were mixed in 20 mL of acetonitrile and

DOI: https://doi.org/10.25077/jrk.v14i2.622

stirred until homogeneous. The 1-methyl-3-propylimidazolium iodide (MPII) 0.4 M was added to the electrolyte to increase conductivity [26]. The electrolyte solution was stored in a dark, closed bottle before being used.

Cell assembly

The photoanode was immersed in 5 g/L bixin solution (in acetone) for 24 hours. One drop of electrolyte was added to the photoanode; then, it was covered with cathode to form a sandwich-like layer. The performance of each cell in the form of short circuit current (I_{SC}) and open circuit voltage (V_{OC}) values were tested using an Agilent 34461 A 6,5 digits scientific multimeter. The light source used in the test was a 500 W halogen lamp. The test conditions were carried out with variation in light intensity form 0 to 1000 W/m^2.

Results and Discussion

Preparation of bixin

Fig. 1 shows the results of TLC analysis of standard bixin, crude extract, and partitioned extract with n-hexane followed by methanol. The eluent used was a mixture of n-hexane and ethyl acetate with a volume ratio of 6:4. The crude extract (Fig. 1b) shows the complexity of the compounds contained in the annatto seeds. Meanwhile, the partitioned extract (Fig. 1c) shows a single spot with the same Rf value as the standard bixin (Rf = 0.32) (Fig. 1a), indicating that bixin was successfully obtained in this work.

The results of UV-Vis spectrophotometry analysis, as presented in Fig. 2, show typical spectra for the bixin molecule in the wavelength range of 400-500 nm.

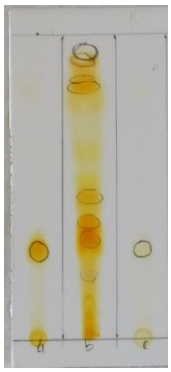

Figure 1. TLC result of standard bixin (a), crude extract (b), and partitioned extract with n-hexane followed by methanol (c)

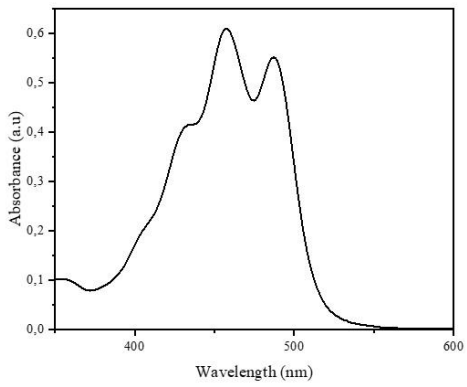

Figure 2. Spectrum of bixin in acetone

This is in line with Rahmalia et al. [26], who reported that bixin (in acetone) has strong absorption in the 400-500 nm wavelength region. This is because bixin has a conjugated double bond as a chromophore group which will produce strong absorption spectra characteristics at wavelengths above 400 nm. Three absorption peaks were observed at 487, 458, and 430 nm. This is almost the same as the report of Rahmalia et al. [27], that bixin with a purity of 81.30%, has three absorption peaks at wavelengths of 487, 458, and 430 nm.

The absorption spectra of bixin, as shown in Fig. 2 show the absorption band according to the transition energy of the carotenoid pigment, namely the electronic transition $\pi \rightarrow \pi^*$ equivalent to S0 → S2. In this case, S0 represents the ground state, S1 is the lowest excited state, and S2 is the second excited state. The three absorption peaks of the carotenoids correspond to the three lowest vibrational bands of the S0 → S2 electronic transition called 0-0, 0-1, and 0-2 [28].

The spectral fine structure or ratio %III/II (the height of the longest-wavelength absorption peak to the middle absorption peak) in carotenoids is one of the analytical methods that can be used to identify the chromophore characteristics of carotenoid compounds [29]. The peak ratio of %III/II bixin in this study was 51.02% where this value is close to the peak ratio of %III/II pure bixin in the study of Rahmalia et al. [25], which was equal to 51.89%.

Characteristic of TiO_2 and Mg-TiO_2 prepared by the hydrothermal method

The photoanode is a thin porous film of metal oxide semiconductor supported onto a transparent conducting oxide (TCO) glass. Modification of photoanode has proven to be a very functional approach for improving DSSC performance. In this work, we synthesized TiO_2 and Mg-doped TiO_2 using TTIP by hydrothermal method.

X-ray diffraction (XRD) test on undoped TiO_2 and Mg-doped TiO_2 was carried out to determine crystallinity, crystal size, and crystal lattice parameters. Based on the diffractogram in Fig. 3, undoped TiO_2 has a diffraction peak of 2θ at 25.24; 38.02, and 48.07°, which correspond to hkl (101), (200), and (211) (JCPDS No. 21-1272). They are characteristic of the crystalline phase of tetragonal anatase. The anatase phase is advantageous for photoanode applications in the DSSC system because it converts solar energy better than the rutile and brookite phases [30]–[32]. Rahmalia et al. [27]. have also investigated that TiO_2 anatase surface can absorb bixin better than TiO_2 P25. There is no rutile and brookite peaks found in all diffractogram. It is indicated that hydrothermal method is being a proper method to produce the anatase crystal type. The same result was also reported by many researchers [33],[34].

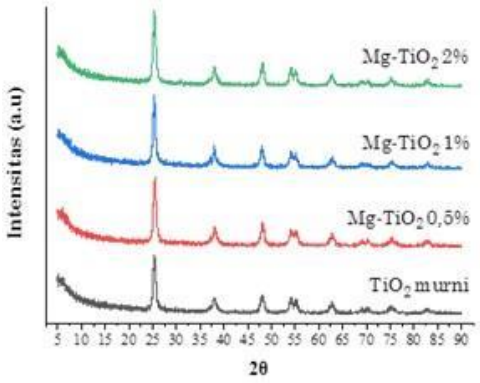

Figure 3. X-ray diffractogram of TiO_2 and Mg-TiO_2

DOI: https://doi.org/10.25077/jrk.v14i2.622

Table 1. Crystal size and lattice of TiO_2; Mg-TiO_2 0.5%; Mg-TiO_2 1% and Mg-TiO_2 2%

No	Material	Crystallite size (nm)	d-spacing (nm)
1.	TiO_2	33.257	0.259
2.	Mg-TiO_2 0.5%	30.770	0.259
3.	Mg-TiO_2 1%	27.561	0.258
4.	Mg-TiO_2 2%	22.704	0.258

No significant difference was observed between the Mg-doped TiO_2 and undoped TiO_2 diffractograms, but the resulting 2θ shift could indicate Mg insertion to TiO2. Mg-TiO_2 with a dopant concentration of 0.5% showed diffraction peaks at 2θ, namely 25.34, 38.09, and 48.04°. Mg- TiO_2 with 1% dopant concentration showed diffraction peaks at 2θ, namely 25.58, 37.91, and 48.15°. Mg-TiO_2 with a dopant concentration of 2% showed diffraction peaks at 2θ, namely 25.50, 38.21, and 48.17°. The diffraction peak of Mg^{2+} was not observed in the diffractogram. This was presumably because the concentration of Mg^{2+} used was too small. The diffraction peaks shift was caused by the change in the distance between the crystal lattices.

The diffraction peaks with the highest intensity were then analyzed using the Debye-Scherrer equation to determine the size of the crystallites. At the same time, the distance between the lattices was determined using Bragg's Law. The calculation results in Table 1 show that the crystallite size and the distance between the Mg-doped TiO_2 lattices decreased although not significant with the increased Mg dopant concentration. This value is much smaller than TiO_2 without dopants. Following the equation $2d_{hkl} \sin\theta = n\lambda$, with the increasing value of θ, the value of d indicates the distance between the planes will be smaller. This indicates that the growth of the TiO_2 crystal matrix was limited by Mg [35].

The analysis using XRD showed that TiO_2 anatase containing Mg was always formed in all compositions, and the absence of peaks of other compounds indicated that the TiO_2 annealing process was successful. This indicates that Mg has been doped into the TiO2 crystal lattice without changing the anatase structure. The higher intensity of Mg- TiO_2 diffraction peaks than pure TiO_2 indicates that adding Mg dopant can increase the crystallinity of TiO_2. The hydrothermal process will cause the interaction between the reactants to be perfect, and the formation of crystal nuclei will take place optimally so that the product is crystalline.

The synthesized TiO_2 and Mg- TiO_2 materials were also characterized using UV-Vis DRS to determine their absorption characteristics and band gap energy (Egap). Band gap energy affects the excitation of electrons from the valence band to the conduction band. When a semiconductor is energized, electrons will be excited to the conduction band leaving a positive charge called holes. Most electron-hole pairs will survive on the surface of the semiconductor, so the holes can work by initiating oxidation reactions and electrons initiating the reduction reactions of chemical compounds around the TiO_2 surface. If the band gap energy is small, the light energy needed is also small. The results of determining the Egap value using the Tauc Plot method are presented in Table 2. The wavelength value was obtained from the Egap conversion using the Planck equation ($E = h. c/\lambda$), where the energy (E) is directly proportional to the Planc constant (h) and the speed of light (c), but inversely proportional to the wavelength (λ).

Table 2. . The band gap energy value and the maximum absorption wavelength of TiO_2, Mg-TiO_2 0.5%, Mg-TiO_2 1%, and Mg-TiO_2 2%

No	Material	Band gap energy (eV)	Wavelength (nm)
1.	TiO_2	3.26	381
2.	Mg-TiO_2 0.5%	2.90	428
3.	Mg-TiO_2 1%	2.72	456
4.	Mg-TiO_2 2%	2.60	477

Based on Table 2, the band gap energy of TiO_2 decreases as the concentration of Mg dopant increases. This is because of the effect of adding Mg metal to the TiO_2 crystal lattice. Mg metal can be inserted into the TiO_2 crystal lattice because the ionic radius of Mg^{2+} (0.57Å) is smaller than the ionic radius of Ti^{4+} (0.68) [36]. In addition, Mg has a lower conduction band than TiO_2, which can cause a decrease in the TiO_2 conduction band. In this case, doping caused the formation of additional states, between conduction band and valence band of TiO_2 [36], have reported that doping induced to sp-d interaction between the band electrons of TiO_2 and dopant d electrons that are localized. In the other study, Ünlü & Ozacar [12], have investigated that more dopant cations cause to creation of impurity states below the conduction band of TiO_2, hence it can be seen that band gap energy were decreased in response to increase at dopant amount. As the band gap energy decreases, the light energy (photons) required to excite electrons from the valence band to the conduction band will be smaller. This is in accordance with the definition of band energy, namely the minimum energy required for electrons from the valence band to be excited in the conduction band of a material.

The decrease in band gap energy also affects the maximum absorption wavelength of TiO_2, which is increasingly shifted towards the wavelength of visible light absorption, which can increase the photon absorption process. This shows that the presence of Mg doping can increase the effectiveness of TiO_2 photovoltaic, which initially only absorbs photon energy in the UV region with a wavelength range of 290-400 nm and can only utilize about 3-5% of the total solar radiation that reaches the earth's surface [37]. The decreasing the band gap energy will widen the TiO_2 absorption band area towards visible light wavelengths, so that when applied to DSSC systems it will increase the efficiency of converting light energy into electrical energy.

DSSC performance

In this study, the performance of DSSC was observed from the values of open-circuit voltage (Voc) and short-circuit current (Isc) produced by cells when exposed to polychromatic light at various light intensities. Voc is the maximum voltage generated by the cell when the current is equal to zero, while Isc is the current value produced by the cell when the voltage is equal to zero. These two values are essential parameters that determine the performance of DSSC [8]. The maximum energy conversion efficiency describes the performance of a DSSC, how much solar energy (photons) can be converted into electrical energy without considering the value of the fill factor. It is the ratio between power generated by DSSC and the power of the light sources [26].

The maximum energy conversion efficiency (η) can be mathematically calculated using equation 1:

$$\eta \max(\%) = \frac{V_{OC} \times I_{SC}}{\text{light intensity}} \times 100\% \quad (1)$$

Variation of light intensity was given to determine the optimum light intensity where the cell shows the best performance.

 DOI: https://doi.org/10.25077/jrk.v14i2.622

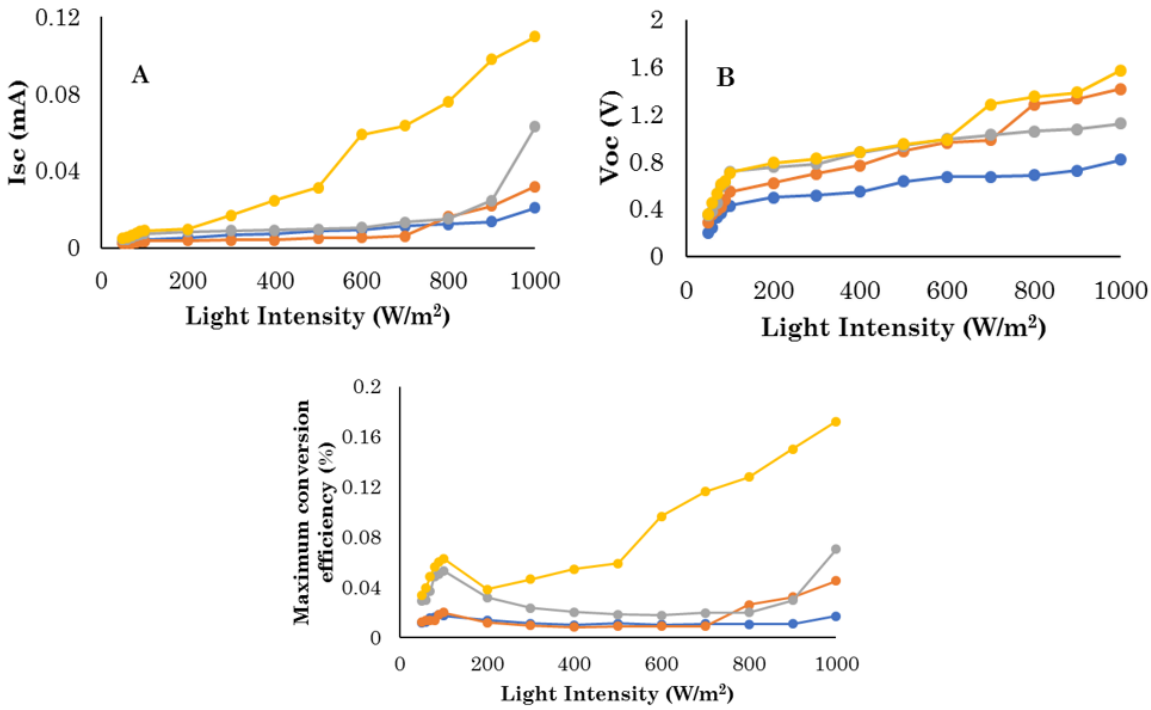

Figure 4. Parameters affecting DSSCs performance using undoped TiO_2 and Mg-TiO_2

Fig. 4a and 4b show that the I_{SC} and V_{OC} values increase with increasing light intensity. The higher the light intensity, the more photons are received by cell, resulting in faster electrons that can be excited from the highest occupied molecular orbital (HOMO) to the lowest unoccupied molecular orbital (LUMO). In effect, the filling of holes in the HOMO orbitals by electrons from the electrolyte will be relatively faster [6],[21].

The presence of Mg dopants in the TiO_2 photoanode causes an increase in I_{SC} and V_{OC} values. DSSC with 2% Mg- TiO_2 photoanode experienced the highest increase in I_{SC} compared to other TiO_2 variations. This was also indicated by the higher V_{OC} value in DSSC with Mg- TiO_2 photoanode than pure TiO_2. In this study, the V_{OC} value with Mg- TiO_2 2% photoanode was the highest compared to pure TiO_2, Mg- TiO_2 0.5%, and Mg- TiO_2 1%. Low band gap energy will increase injection and electron transport [8],[26]. This increase indicates the role of Mg dopant in TiO_2 photoanode.

The maximum energy conversion efficiency DSSC value was achieved at an intensity of 1000 W/cm², which is 0.017; 0.045; 0.070; and 0.172% for cells with undoped TiO_2 photoanode, 0.5% Mg- TiO_2, respectively; Mg-TiO_2 1% and Mg- TiO_2 2%. The effect of the doping on the DDSCs performance parameters is closely related to the electronic structure of the TiO_2 photoanode. The high energy conversion efficiency due to the cell with 2% Mg-doped photoanodes having better photon absorption capabilities due to their smaller band gap energy. Low-efficiency value of DSSC with undoped TiO_2 photoanode was due to the large energy band gap (Egap). Hence, the number of electrons that can move from the valence band to the conduction band when exposed to polychromatic light was less. Similar results have been previously reported by several researchers regarding the effect of band gap on the energy conversion efficiency of DSSC [8][38].

In addition, the maximum conversion efficiency value of DSSC in this study is also higher than that of DSSC using bixin dye and metakaolinite-doped TiO_2 photoanode, which has been carried out by Rahmalia et al. [8], with an efficiency value of 0.086%. Thus, this study

shows that the presence of Mg doping on the TiO2 photoanode can increase the maximum conversion efficiency of bixin-sensitized solar cells.

Conclusions

Mg-doped TiO_2 has better electronic properties than undoped TiO_2. The higher the concentration of dopants, the crystallinity of TiO_2 increases, the band gap energy of TiO_2 decreases until it reaches 2.60 eV, and the wavelength shifts towards visible light. The highest DSSC energy conversion efficiency was obtained at a dopant concentration of 2%, which is around 0.1719%. The greater the intensity of light hitting the DSSC, the greater the value of the short circuit current (I_{SC}), open circuit voltage (V_{OC}), and the maximum energy conversion efficiency obtained by the DSSC. The efficiency of DSSC increases as the energy gap decreases.

Acknowledgments

This study received financial support from the Ministry of Research Technology and the Higher Education Republic of Indonesia (KEMENTRISTEK DIKTI) through the National Competitive Research (058/E4.1/AK.04.PT/DRPM/2021).

References

1. Tontapha, S., Uppachai, P. & Amornkitbamrung, V., Fabrication of Functional Materials for Dye-sensitized Solar Cells. *Front. Energy Res.*, **9(April)**: 1–9 (2021).
2. Ananth, S., Vivek, P., Saravana Kumar, G. & Murugakoothan, P., Performance of Caesalpinia sappan heartwood extract as photo sensitizer for dye sensitized solar cells. *Spectrochim. Acta - Part A Mol. Biomol. Spectrosc.*, **137**: 345–350 (2015).
3. Sharma, K., Sharma, V. & Sharma, S. S., Dye-Sensitized Solar Cells: Fundamentals and Current Status. *Nanoscale Res. Lett.*, **13**: (2018).
4. Alazoumi, S., Elhub, B., Awsha, A. A., Alazoumi, S. H. & Elhub, B., A Review on the development of TiO2 photoanode for Solar Applications. *Albahit J. Appl. Sci.*, **2(2)**: 9–9 (2021).
5. Ruhane, T. A., Islam, M. T., Rahaman, M. S., Bhuiyan, M. M. H., Islam, J. M. M., Newaz, M. K., Khan, K. A., *et al.*, Photo current enhancement of natural dye sensitized solar cell by optimizing dye extraction and its loading period. *Optik (Stuttg).*, **149**: 174–183 (2017).
6. Khan, M. I., Farooq, W. A., Saleem, M., Bhatti, K. A., Atif, M. & Hanif, A., Phase change, band gap energy and electrical resistivity of Mg doped TiO2 multilayer thin films for dye sensitized solar cells applications. *Ceram. Int.*, **45(17)**: 21436–21439 (2019).
7. Cui, Y., Zhang, L., Lv, K., Zhou, G. & Wang, Z. S., Low temperature preparation of TiO2 nanoparticle chains without hydrothermal treatment for highly efficient dye-sensitized solar cells. *J. Mater. Chem. A*, **3(8)**: 4477–4483 (2015).
8. Rahmalia, W., Silalahi, I. H., Usman, T., Fabre, J. F., Mouloungui, Z. & Zissis, G., Stability, reusability, and equivalent circuit of TiO2/treated metakaolinite-based dye-sensitized solar cell: effect of illumination intensity on V oc and I sc values. *Mater. Renew. Sustain. Energy*, **10(2)**: 1–10 (2021).
9. Widiatannur, U., Usman, T. & Rahmalia, W., 555-1711-1-Pb (1). **05(2655)**: (2020).
10. Neetu., Singh, S., Srivastava, P. & Bahadur, L., Hydrothermal synthesized Nd-doped TiO2 with Anatase and Brookite phases as highly improved photoanode for dye-sensitized solar cell. *Sol. Energy*, **208(July)**: 173–181 (2020).
11. Prakash, J., Samriti., Kumar, A., Dai, H., Janegitz, B. C., Krishnan, V., Swart, H. C., *et al.*, Novel rare earth metal–doped one-dimensional TiO2 nanostructures: Fundamentals and multifunctional applications. *Mater. Today Sustain.*, **13**: 100066 (2021).

 DOI: https://doi.org/10.25077/jrk.v14i2.622

12. Ünlü, B. & Özacar, M., Effect of Cu and Mn amounts doped to TiO2 on the performance of DSSCs. *Sol. Energy*, **196(October 2019)**: 448–456 (2020).

13. Shakir, S., Abd-ur-Rehman, H. M., Yunus, K., Iwamoto, M. & Periasamy, V., Fabrication of un-doped and magnesium doped TiO2 films by aerosol assisted chemical vapor deposition for dye sensitized solar cells. *J. Alloys Compd.*, **737**: 740–747 (2018).

14. Lv, C., Lan, X., Wang, L., Yu, Q., Zhang, M., Sun, H. & Shi, J., Alkaline-earth-metal-doped TiO2 for enhanced photodegradation and H2 evolution: Insights into the mechanisms. *Catal. Sci. Technol.*, **9(21)**: 6124–6135 (2019).

15. Athira, K., Merin, K. T., Raguram, T. & Rajni, K. S., Synthesis and characterization of Mg doped TiO2nanoparticles for photocatalytic applications. *Mater. Today Proc.*, **33(xxxx)**: 2321–2327 (2020).

16. Mursal., Malahayati., Azmi, N. & Fatmiyah, S., Synthesis of TiO2-based photoelectrode and natural dye for dye sensitized solar cell (DSSC). *J. Phys. Conf. Ser.*, **1882(1)**: (2021).

17. Wahab, H. S. & Hussain, A. A., Photocatalytic oxidation of phenol red onto nanocrystalline TiO2 particles. *J. Nanostructure Chem.*, **6(3)**: 261–274 (2016).

18. Nam, T. Van., Trang, N. & Cong, B., Mg-doped TiO2 for dye-sensitive solar cell: An electronic structure study. *Proc. Natl. Conf. Theor. Phys*, **37**: 233–242 (2012).

19. Zhang, R., Zhou, Y., Peng, L., Li, X., Chen, S., Feng, X., Guan, Y., *et al.*, Influence of SiO2 shell thickness on power conversion efficiency in plasmonic polymer solar cells with Au nanorod@SiO 2 core-shell structures. *Sci. Rep.*, **6(January)**: 1–9 (2016).

20. Karkare, M. M., Choice of precursor not affecting the size of anatase TiO2 nanoparticles but affecting morphology under broader view. *Int. Nano Lett.*, **4(3)**: (2014).

21. Liu, J., Yang, H., Tan, W., Zhou, X. & Lin, Y., Photovoltaic performance improvement of dye-sensitized solar cells based on tantalum-doped TiO2 thin films. *Electrochim. Acta*, **56(1)**: 396–400 (2010).

22. Giridhar, P. Venugopalan, A. Parimalan, R., A Review on Annatto Dye Extraction, Analysis and Processing – A Food Technology Perspective. *J. Sci. Res. Reports*, **3(2)**: 327–348 (2014).

23. Rios, A. D. O., Borsarelli, C. D. & Mercadante, A. Z., Thermal degradation kinetics of bixin in an aqueous model system. *J. Agric. Food Chem.*, **53(6)**: 2307–2311 (2005).

24. Gómez-Ortíz, N. M., Vázquez-Maldonado, I. A., Pérez-Espadas, A. R., Mena-Rejón, G. J., Azamar-Barrios, J. A. & Oskam, G., Dye-sensitized solar cells with natural dyes extracted from achiote seeds. *Sol. Energy Mater. Sol. Cells*, **94(1)**: 40–44 (2010).

25. Rahmalia, W., Septiani., Naselia, U. A., Usman, T., Silalahi, I. H. & Mouloungui, Z., Performance improvements of bixin and metal-bixin complexes sensitized solar cells by 1-methyl-3-propylimidazolium iodide in electrolyte system. *Indones. J. Chem.*, **21(3)**: 669–678 (2021).

26. Rahmalia, W., Fabre, J. F., Usman, T. & Mouloungui, Z., Aprotic solvents effect on the UV-visible absorption spectra of bixin. *Spectrochim. Acta - Part A Mol. Biomol. Spectrosc.*, **131**: 455–460 (2014).

27. Rahmalia, W., Fabre, J.-F. & Mouloungui, Z., Effects of Cyclohexane/Acetone Ratio on Bixin Extraction Yield by Accelerated Solvent Extraction Method. *Procedia Chem.*, **14**: 455–464 (2015).

28. Llansola-Portoles, M. J., Pascal, A. A. & Robert, B., Electronic and vibrational properties of carotenoids: From in vitro to in vivo. *J. R. Soc. Interface*, **14(135)**: (2017).

29. Rodriguez, D., *A Guide to Carotenoid Analysis in Foods*. *Life Sciences*, (2001).

30. Rahimi, N., Pax, R. A. & Gray, E. M. A., Review of functional titanium oxides. I: TiO2 and its modifications. *Prog. Solid State*

Chem., **44(3)**: 86–105 (2016).

31. Kim, B. M., Rho, S. G. & Kang, C. H., Effects of TiO 2 structures in dye-sensitized solar cell. *J. Nanosci. Nanotechnol.*, **11(2)**: 1515–1517 (2011).
32. Mousa, M. A., Khairy, M. & Mohamed, H. M., Dye-Sensitized Solar Cells Based on an N-Doped TiO2 and TiO2-Graphene Composite Electrode. *J. Electron. Mater.*, **47(10)**: 6241–6250 (2018).
33. Kumar, N., Hazarika, S. N., Limbu, S., Boruah, R., Deb, P., Namsa, N. D. & Das, S. K., Hydrothermal synthesis of anatase titanium dioxide mesoporous microspheres and their antimicrobial activity. *Microporous Mesoporous Mater.*, **213**: 181–187 (2015).
34. Ulhaq, M. R. & Kusumawardani, C., The Effect of the Hydrothermal Time and Temperature in the Synthesis to the Properties of Nitrogen-doped TiO2. *Indones. J. Chem. Environ.*, **5(1)**: 17–24 (2022).
35. Eka Sri Kunarti, et. a., Pengujian Aktivitas Komposit Fe2O3-SiO2 Sebagai Fotokatalis Pada Fotodegradasi 4-Klorofenol. *Manusia dan Lingkungan. Kimia FMIPA UGM. Yogyakarta*, **16(Maret)**: 54–64 (2009).
36. Zhang, J., Peng, W., Chen, Z., Chen, H. & Han, L., Effect of cerium doping in the TiO 2 photoanode on the electron transport of dye-sensitized solar cells. *J. Phys. Chem. C*, **116(36)**: 19182–19190 (2012).
37. Yacoubi, B., Samet, L., Bennaceur, J., Lamouchi, A. & Chtourou, R., Materials Science in Semiconductor Processing Properties of transition metal doped-titania electrodes : Impact on efficiency of amorphous and nanocrystalline dye-sensitized solar cells. *Mater. Sci. Semicond. Process.*, **30**: 361–367 (2015).
38. Ahmed, M. I., The Effect of Optical Energy Gaps on the Efficiency for Dye Sensitized Solar Cells (DSSC) by using Gum Arabic Doped by CuO and (Coumarin 500 , Ecrchrom Black , Rhodamin B and DDTTc) Dyes. **(December)**: (2019).

 DOI: https://doi.org/10.25077/jrk.v14i2.622